

# Supplementary Information

## Influence of oversized cations on electronic dimensionality of d-MAPbI<sub>3</sub> crystals

Mateusz Dyksik,<sup>\*,†,‡</sup> Michal Baranowski,<sup>†,‡</sup> Antonin Leblanc,<sup>¶</sup> Alessandro Surrente,<sup>†</sup> Miriam Karpińska,<sup>§</sup> Joanna M. Urban,<sup>†</sup> Łukasz Kłopotowski,<sup>§</sup> Duncan K. Maude,<sup>†</sup> Nicolas Mercier,<sup>¶</sup> and Paulina Plochocka<sup>\*,†,‡</sup>

<sup>†</sup>*Laboratoire National des Champs Magnétiques Intenses, UPR 3228,  
CNRS-UGA-UPS-INSA, Grenoble and Toulouse, France*

<sup>‡</sup>*Department of Experimental Physics, Faculty of Fundamental Problems of Technology,  
Wroclaw University of Science and Technology, Wroclaw, Poland*

<sup>¶</sup>*MOLTECH ANJOU, UMR-CNRS 6200, Université d'Angers, 2 Bd Lavoisier, 49045  
Angers, France*

<sup>§</sup>*Institute of Physics, Polish Academy of Sciences, 02-668 Warsaw, Poland*

E-mail: mateusz.dyksik@pwr.edu.pl; paulina.plochocka@lncmi.cnrs.fr

## 1 Intensity of optical transitions from reflectance spectra

In the main text we present a comparison of the intensity of the low and high energy transitions (see Fig. 2d). To determine these quantities we calculated the modulus spectrum  $M(E)$ ,  $M(E) = \sqrt{[R(E)]^2 + [I(E)]^2}$ , where  $R(E)$  is the measured reflectance spectrum (or its derivative).<sup>1,2</sup>  $I(E)$  is calculated from  $R(E)$  by means of the Kramers-Kronig relations. Figure S1 shows both the reflectance derivative and  $M(E)$  spectrum for the  $x = 15\%$  sample. The intensity of the low and high energy region was calculated taking the respective area under the  $M(E)$  spectrum.

In order to apply the Kramers-Kronig relations to obtain  $I(E)$ , the following conditions have to be fulfilled: (i) the sample under investigation has to be semi-infinite; (ii) the reflectance spectrum has to be measured at normal incidence; (iii)  $R(E)$  has to be zero at the boundary to avoid the extrapolation problem.<sup>3</sup> Since in our work we measure reflectance spectra of crystals at a perpendicular incidence in a broad spectral range all these criteria are met.

## 2 Extracting transition energies from reflectance spectra

To determine the transition energy  $E_0$  of the high energy features from the reflectance derivative  $\frac{dR}{dE}$  spectra, we fitted the solid points in Fig. 2(a) with the following formula:<sup>4</sup>

$$\frac{dR}{dE} = \Re[Ce^{i\phi}(E - E_0 + i\Gamma)^{-n}], \quad (1)$$

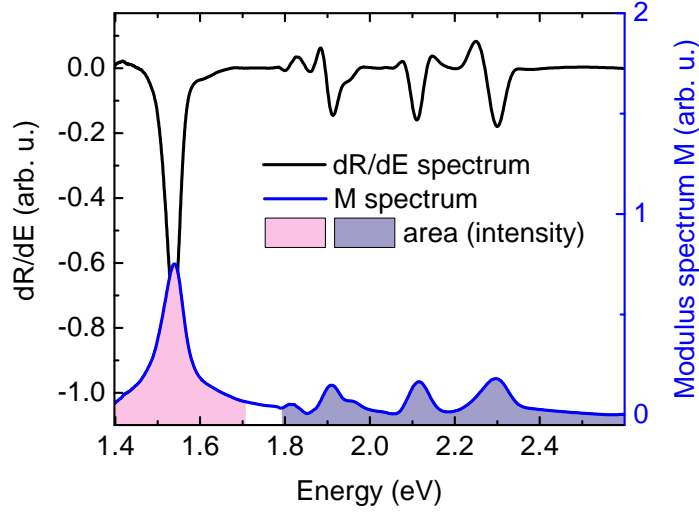


Figure S1: Reflectance derivative spectrum (black curve) and modulus spectrum (blue curve) of the  $x = 15\%$  d-MAPbI<sub>3</sub>

where  $C$  is the amplitude,  $\phi$  the phase angle,  $E$  the photon energy and  $\Gamma$  the broadening parameter. The parameter  $n$  determines the line shape. For  $n = 2$ , Eq. (1) corresponds to the derivative of a Lorentzian function. For  $n = 3$ , it mimics the derivative of a Gaussian function. As we show in Fig. 2(a) of the main text, fitting Eq. (1) with  $n = 3$  reproduces well the experimental data points.

### 3 Photoluminescence spectrum of lead deficient MAPbI<sub>3</sub>

Fig. S2 shows a comparison of the PL spectrum of the three samples under investigations with the concentration of Pb-I vacancies of 13, 15 and 20%. Similar to the reflectance derivative spectra presented in the main text (see Fig. 2(b)), the influence of the oversized cations is clearly visible. For an increasing concentration of vacancies, the intensity of the low energy transition (corresponding to the bulk-like phase) quenches. At the same time, the high energy transitions (corresponding to regions with a reduced dimensionality) gain in intensity.

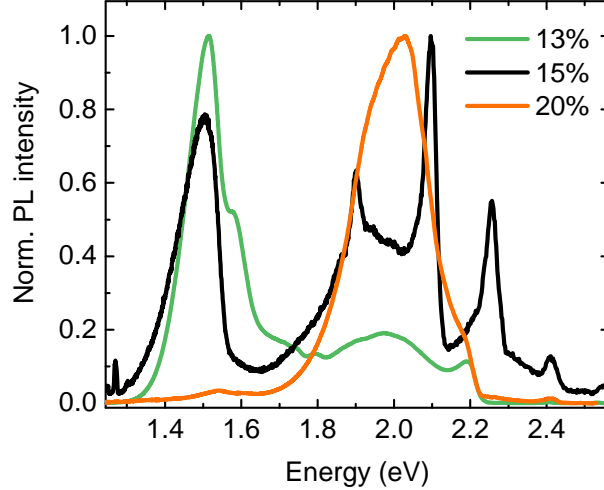


Figure S2: PL spectra of all the investigated samples.

## 4 Comparison of d-MAPbI<sub>3</sub> with 2D perovskites

Fig. S3 compares the PL spectrum of the  $x = 15\%$  d-MAPbI<sub>3</sub> with the PL spectra of 2D perovskites with different number  $n$  of octahedra layers ((MA) <sub>$n-1$</sub> Pb <sub>$n$</sub> I <sub>$3n+1$</sub>  2D perovskite,  $n=1,2$  and 3, after Ref.<sup>5</sup>). Intriguingly, the high energy peaks of the PL spectrum of d-MAPbI<sub>3</sub> have an energy close to the excitonic peaks of Ruddlesden Popper perovskites of different thickness.

## 5 Diamagnetic shift of optical transitions of d-MAPbI<sub>3</sub>

In order to determine the diamagnetic coefficients  $c_0$  presented in Fig. 3(d) of the main text, the data points from Fig. 3(c) were fitted with the  $\Delta E = c_0 B^2$  (see Eq. (1) of the main text). The fitting curves are presented in Fig. S4 in gray for both low and high energy transitions.

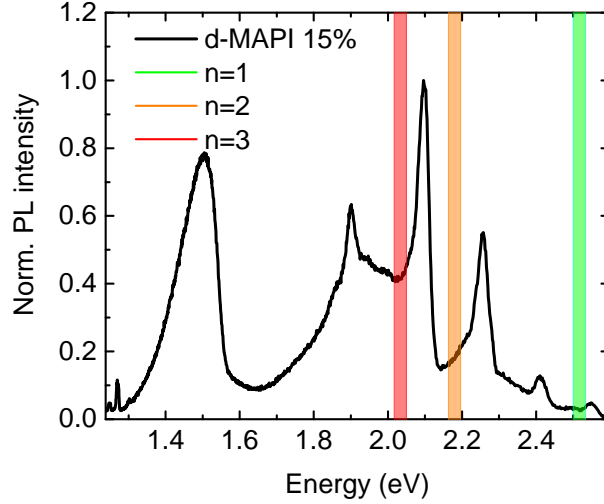


Figure S3: Comparison of the PL spectrum of the  $x = 15\%$  d-MAPbI<sub>3</sub> sample with the main excitonic peak observed for the 2D perovskites with a varying thickness of the inorganic slab.<sup>5</sup>

## 6 Reconstruction of PL lifetime distribution with the Maximum Entropy Method

The measured PL traces for all the investigated samples exhibit a strongly non-exponential behaviour. In order to determine the PL lifetime, in particular the short-lifetime component governing the decay of PL intensity during the first  $\sim 10$  ns after the optical excitation, we used the Maximum Entropy Method.<sup>6</sup> The method fulfills two constraints: (i) the maximization of the Shannon-Jaynes entropy function<sup>7</sup> and (ii) the minimization of the Pearson  $\chi^2$  goodness-of-fit function. The algorithm by Skilling and Bryan,<sup>8</sup> taking into account these two criteria, converges to the optimum distribution of lifetimes, which represents the data adequately ( $\chi^2 \sim 0$ ). In order to compare the lifetime distributions of different PL traces, the same parameters were chosen for each reconstruction ( $0.5 \text{ ns} < \tau < 200 \text{ ns}$ , number of lifetimes  $N = 200$ ).

Fig. S5 (a) and (b) show the PL traces for samples with  $x=13$  and  $15\%$ , respectively (a similar analysis is shown in the main text for the  $x = 15\%$  sample). In both figures the reddish and blueish data points correspond to the low and high energy optical transition, respectively.

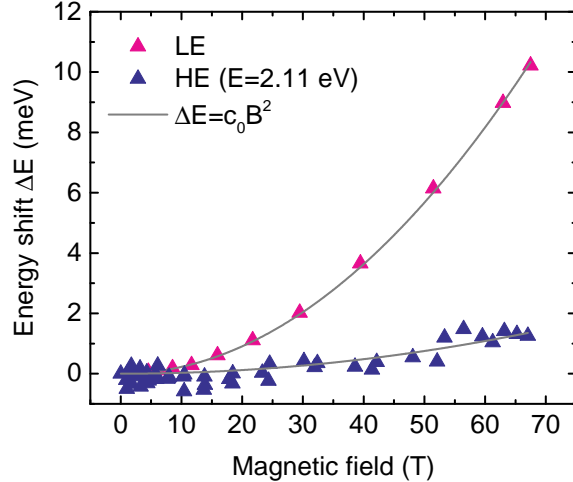


Figure S4: Diamagnetic shifts of the low energy (LE, red triangles) and high energy (HE, blue triangles) transitions measured in the  $x = 15\%$  d-MAPbI<sub>3</sub> sample.

Figures S5 (c) and (d) show the lifetime distributions obtained via the Maximum Entropy Method. All the investigated samples exhibit a similar trend: the distribution describing the PL decay of the high energy transition peaks at a shorter lifetime as compared to that of the PL decay of the 3D-like transition (for  $x = 13\%$ ,  $\tau_{LD} = 0.75$  ns ,  $\tau_{3D} = 4.6$  ns ; for  $x = 20\%$ ,  $\tau_{LD} = 0.72$  ns ,  $\tau_{3D}$  not possible to resolve due to low PL yield, see Fig. S2).

## 7 Crystal synthesis

All materials were prepared with lead iodide 99% (Sigma-Aldrich), methylamine solution 40% in water (Sigma-Aldrich), ethanolamine purified by recrystallisation 99.5% (Sigma-Aldrich), hydroiodic acid 57% in water (Sigma-Aldrich). Crystals of d-HPs (MA,HEA)<sub>1+x</sub>Pb<sub>1-x</sub>I<sub>3-x</sub> ( $x = 13, 15, 20\%$ ) were synthesized by a liquid-gas slow diffusion method. Lead iodide (300 mg) was first dissolved into hydroiodic acid (1.5 mL), in which both methylamine and ethanolamine were added in a second step (ethanolamine/methylamine/lead iodide stoichiometry of 1.5/2/3, 2/2/3 and 3/2/3  $x=13, 15$  and  $20\%$ , respectively). The solution was stirred during 20 minutes, at room temperature, until complete dissolution. This saturated solution was placed into a saturated ethanol vapor atmosphere. After 2 days, red ( $x = 20\%$ )

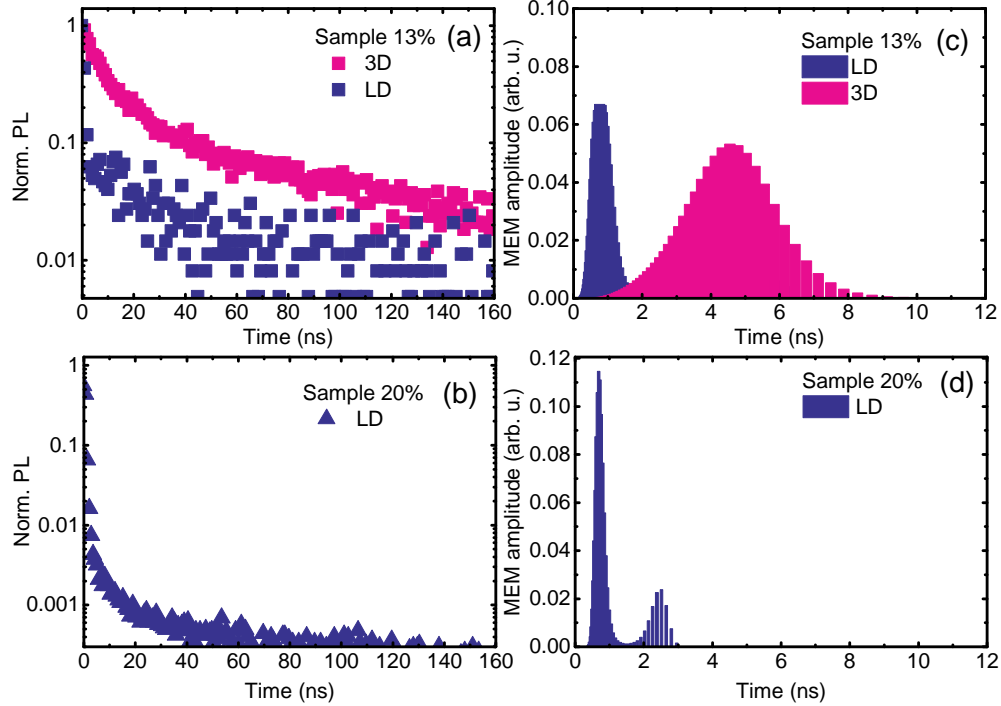


Figure S5: Decay curves (a, b) and distribution of the life times (c, d) for the  $x = 13\%$  and  $x = 20\%$  samples.

or black ( $x=13\%$ ,  $15\%$ ) crystals were obtained and washed 3 times by ethyl acetate and heated at  $60^\circ\text{C}$  during 20 minutes.

## References

- (1) Hosea, T. J. C. Estimating Critical-Point Parameters of Modulated Reflectance Spectra. *physica status solidi (b)* **1995**, *189*, 531–542.
- (2) Jezierski, K.; Markiewicz, P.; Misiewicz, J.; Panek, M.; Ściana, B.; Korbutowicz, R.; Tl/aczal/a, M. Application of Kramers–Krönig analysis to the photoreflectance spectra of heavily doped GaAs/SI-GaAs structures. *Journal of Applied Physics* **1995**, *77*, 4139–4141.
- (3) Jezierski, K. Improvements in the Kramers-Kronig analysis of reflection spectra. *Journal of Physics C: Solid State Physics* **1986**, *19*, 2103–2112.

- (4) Aspnes, D. Third-derivative modulation spectroscopy with low-field electroreflectance. *Surface Science* **1973**, *37*, 418–442.
- (5) Blancon, J.-C.; Stier, A. V.; Tsai, H.; Nie, W.; Stoumpos, C.; Traore, B.; Pedesseau, L.; Kepenekian, M.; Katsutani, F.; Noe, G. et al. Scaling law for excitons in 2D perovskite quantum wells. *Nature communications* **2018**, *9*, 2254.
- (6) Swaminathan, R.; Periasamy, N. Analysis of fluorescence decay by the maximum entropy method: Influence of noise and analysis parameters on the width of the distribution of lifetimes. *Proceedings of the Indian Academy of Sciences: Chemical Sciences* **1996**, *108*, 39–49.
- (7) Shaver, J. M.; McGown, L. B. Maximum Entropy Method for Frequency Domain Fluorescence Lifetime Analysis. 1. Effects of Frequency Range and Random Noise. *Analytical Chemistry* **1996**, *68*, 9–17.
- (8) Skilling, J.; Bryan, R. K. Maximum entropy image reconstruction: general algorithm. *Monthly Notices of the Royal Astronomical Society* **1984**, *211*, 111–124.